

---

# Context parrotting: A simple but tough-to-beat baseline for foundation models in scientific machine learning

---

**Yuanzhao Zhang**

Santa Fe Institute

Santa Fe, NM, USA

[yzhang@santafe.edu](mailto:yzhang@santafe.edu)

**William Gilpin**

University of Texas at Austin

Austin, TX, USA

[gilpin@chaos.utexas.edu](mailto:gilpin@chaos.utexas.edu)

## Abstract

Recently-developed time series foundation models for scientific machine learning exhibit emergent abilities to predict physical systems. These abilities include zero-shot forecasting, in which a model forecasts future states of a system given only a short trajectory as context. Here, we show that foundation models applied to physical systems can give accurate predictions, but that they fail to develop meaningful representations of the underlying physics. Instead, foundation models often forecast by context parrotting, a simple zero-shot forecasting strategy that copies directly from the context. As a result, a naive direct context parrotting model scores higher than state-of-the-art time-series foundation models on predicting a diverse range of dynamical systems, at a tiny fraction of the computational cost. We draw a parallel between context parrotting and induction heads, which explains why large language models trained on text can be repurposed for time series forecasting. Our dynamical systems perspective also ties the scaling between forecast accuracy and context length to the fractal dimension of the attractor, providing insight into the previously observed in-context neural scaling laws. Context parrotting thus serves as a simple but tough-to-beat baseline for future time-series foundation models and can help identify in-context learning strategies beyond parrotting.

## 1 Introduction

A key test of generalization in scientific machine learning (SciML) is the ability to forecast future states of a new physical system. Prior SciML approaches primarily focused on developing specialized forecasting models trained extensively on specific dynamical systems [1–25]. However, the generality of these models is limited by the amount of system-specific data available, motivating the recent development of time-series foundation models [26–41], which are trained on vast amounts of observed and simulated time series, and which can subsequently perform zero-shot forecasts for any time series—including those generated by previously-unseen dynamical systems. Interestingly, it was recently found that, when available historical data is limited, time-series foundation models outperform classical deep learning models in forecasting chaotic dynamical systems [42].

What mechanisms do time-series foundation models use to make zero-shot forecasts, and why they are effective for dynamical systems? It was recently observed that one such foundation model, Chronos [35], often employs an extremely simple strategy when forecasting chaotic systems [42]. The strategy, *context parrotting*, scans the context for repeating motifs and copies the part of the context following the best-matching motif as its prediction (Fig. 1). This can be viewed as a kind of “in-context nearest neighbor” algorithm, which has zero trainable parameters and thus requires no training. So how good is context parrotting as a zero-shot forecasting strategy on its own?

Here, we compare context parrotting with three state-of-the-art time series foundation models: Chronos [35], TimesFM [37], and TimeMoE [39] on the challenging task of forecasting chaotic systems. We

find that context parroting outperforms all three foundation models in both zero-shot forecast accuracy and inference cost, especially for longer context windows. Our results suggest that current time series foundation models fail to extract physical insight from dynamical systems, and that their apparent performance is largely due to benchmark tasks that may be solved by simple repetition.

Our main contributions are:

1. Introduce context parroting as a simple but tough-to-beat baseline for zero-shot forecasting of dynamical systems
2. Show that context parroting outperforms time-series foundation models in predicting chaotic systems
3. Explain the in-context neural scaling law between forecast accuracy and context length, linking the scaling coefficient to the fractal dimension of the underlying attractor

## 2 Related work

### 2.1 Foundation models for science

Foundation models have recently been introduced for many scientific machine-learning tasks [43], including partial differential equations [44–50], neuroscience [51–53], and weather forecasting [54, 55]. However, most of these foundation models remain a black box and haven’t provided interpretable insights into the underlying process. Here, we analyze context parroting as a simple mechanism coming out of time-series foundation models, noting its strengths and weaknesses as a zero-shot forecasting strategy. This strategy, and the insights gained here, can potentially be applied to other scientific tasks.

### 2.2 In-context neural scaling law

Neural scaling laws describe the relation between the performance of a neural network and certain resources, such as model size, data size, or the amount of compute [56–59]. Such scaling laws allow practitioners to predict the performance of yet-to-be-trained models based on the available resources and allocate them optimally [60].

When applying LLMs to forecast dynamical systems, Liu et al. [61] recently observed an in-context neural scaling law, in which the test loss decreases with the context window following a power law. Here, we show that this in-context neural scaling law can be reproduced when using context parroting to predict dynamical systems, and the scaling coefficient can be linked to an invariant property of the underlying dynamic process (the fractal dimension of the chaotic attractor). This finding shows that neural scaling laws are intrinsically linked to invariant properties of the process generating the data, and the theory can potentially be generalized to other models and tasks (e.g., can we estimate the “fractal dimension” of language from the neural scaling law of LLMs?).

### 2.3 In-context learning and induction heads

Induction heads are computational circuits that naturally emerge in simple transformers through training, and they have been hypothesized to underlie a lot of the in-context learning ability of foundation models [62–64]. In its simplest form, an induction head copies from repeating tokens in the context to make predictions. For example, when presented with a token stream  $[A][B]\dots[A]$ , an induction head will output  $[B]$  as the next token. Prior works train transformers on minimal Markov chain grammars, and find that, during pretraining, models learn to identify increasingly higher-order  $k$ -grams, with different attention heads specializing in copying, lookup, and aggregation [65, 66]. These works imply that pretraining enables models to learn conditional distributions, allowing them to represent sequence distributions seen in the context [67–70].

There is a clear parallel between context parroting and induction heads: both are essentially copy-and-paste operations, with context parroting involving the matching of not just one but multiple tokens. In fact, it is easy to imagine context parroting emerging naturally from combining multiple induction heads. This parallel can potentially explain the unreasonable effectiveness of applying language models trained on text to time-series tasks without fine-tuning or prompt engineering [27, 29–31, 61]. The induction heads formed from training on natural language happen to be also

effective for predicting time series and can be easily repurposed to implement strategies such as context parroting.

### 3 Context parroting as an effective strategy for zero-shot forecasting

**Overview of context parroting.** In this section we motivate and introduce our baseline: context parroting. It was first identified as a strategy used by Chronos to predict chaotic systems, such as the partially observed Lorenz system shown in Fig. 1. It was also shown that one can predict the forecast accuracy of Chronos based on the context trajectory [42]: If there is a motif in the context that closely matches what happened immediately before the prediction starts, then Chronos would do well. This suggests that Chronos heavily utilizes context parroting to forecast chaotic systems. The parroting mechanism also explains Chronos’s sensitivity to initial conditions and sampling rate.

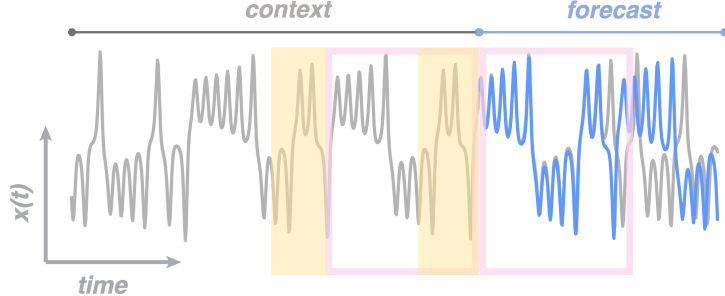


Figure 1: **Example of a foundation model forecasting chaotic dynamics with context parroting.** Here, the foundation model (Chronos) was asked to predict the  $x$  variable of the Lorenz system based on a short context trajectory with 512 data points. Blue is the prediction and gray is the ground truth. Chronos produced an accurate prediction by simply looking for a motif in the context similar to the motif immediately preceding the prediction (highlighted in yellow) and copying the evolution following the matching motif (highlighted by pink boxes). We distill this context parroting strategy into Algorithm 1 and compare it against time-series foundation models (including Chronos itself).

Context parroting is a simple forecasting strategy in which a model uses the last  $D$  tokens of its context to query the remaining context. For whatever context sequence most closely matches the query, the following  $H$  subsequent tokens are copied and used as the forecast. During the matching process, we exclude the last  $D$  motifs to avoid parroting too close to where the prediction starts. Framed in terms of induction heads, the query lookup acts as a *copy* head, the nearest-neighbor match is a *selector*, and the exact repetition is the *aggregation* operation [66]. We describe this approach in Algorithm 1.

---

#### Algorithm 1 Context Parroting

**Input:** Context trajectory  $x_{1:t} = \{x_1, \dots, x_t\}$ , embedding dimension  $D$  and forecast length  $h$ .

**Output:** Forecast trajectory  $x_{t+1:t+h} = \{x_{t+1}, \dots, x_{t+h}\}$ .

- 1: **for all** length- $D$  motif  $s$ :  $x_{s-D+1:s}$  in the context  $x_{1:t-D}$  **do**
- 2:   compute the distance  $d_s$  between motif  $s$  and the last motif  $x_{t-D+1:t}$
- 3:   Find the best-matching motif,  $s_{opt}$ , with the smallest distance
- 4:   Set the first  $t - s_{opt}$  predicted points to be  $x_{t+1:2t-s_{opt}} = x_{s_{opt}+1:t}$  and repeat until the forecast length  $h$  is reached

---

**Mathematical Formulation.** Context parroting corresponds to a continuous 1-nearest-neighbor search over sequences of length  $D$  in the context of length  $L$ . It thus corresponds to a limit of a Nadaraya–Watson model of the time series,

$$\hat{p}(\mathbf{y} \mid \mathbf{q}) = \frac{\sum_{j=D}^{L-H} K_\sigma(\mathbf{q}, \mathbf{x}_{j-(D-1):j}) K_\sigma(\mathbf{y}, \mathbf{x}_{j+1:j+H})}{\sum_{j=D}^{L-H} K_\sigma(\mathbf{q}, \mathbf{x}_{j-(D-1):j})}, \quad (1)$$

where the query  $\mathbf{q}$  represents the length- $D$  motif immediately preceding the end of the context window.  $\mathbf{y}$  represents a length- $H$  forecast of subsequent values. The forecast sequence  $\mathbf{y}$  has probability  $\hat{p}$  conditioned on the query. The symmetric kernel  $K_\sigma(\mathbf{u}, \mathbf{v}) = \sigma^{-d} K((\mathbf{u} - \mathbf{v})/h\sigma)$  has bandwidth  $\sigma$  in dimension  $d = D \cdot \dim(x_t)$ . Assuming mean-squared error as a distance function in sequence space, we use a Gaussian kernel

$$K_\sigma(\mathbf{u}, \mathbf{v}) = \frac{1}{(2\pi\sigma^2)^{d/2}} \exp\left(-\frac{\|\mathbf{u} - \mathbf{v}\|^2}{2\sigma^2}\right)$$

In practice, the second kernel on  $\mathbf{y}$  in Eq. 5 becomes a delta function, and so we write the conditional mean predictor

$$\hat{y}(\mathbf{q}) = \sum_{j=D}^{L-H} w(\mathbf{q}, \mathbf{x}_{j-(D-1):j}) \mathbf{x}_{j+1:j+H}, \quad w(\mathbf{q}, \mathbf{z}) \equiv \frac{K_\sigma(\mathbf{q}, \mathbf{z})}{\sum_{j=D}^{L-H} K_\sigma(\mathbf{q}, \mathbf{x}_{j-(D-1):j})}. \quad (2)$$

Context parroting corresponds to the 1-nearest-neighbor limit  $\sigma \rightarrow 0$ .

**Context parroting preserves attractor properties at long context lengths.** In Appendix C.3, we derive the following proposition,

$$\lim_{L \rightarrow \infty} \mathbb{E}_p[F(\mathbf{y})|\mathbf{q}] = \mathbb{E}_\mu[F(\mathbf{x})]$$

where  $L$  is the context length for an Nadaraya–Watson estimator  $p$ ,  $F(\mathbf{y})$  is an estimate from a forecast sequence  $\mathbf{y}$  of a property  $F$  of an ergodic dynamical system, which has an invariant value  $\mathbb{E}_\mu[F(\mathbf{x})]$  when calculated over the full attractor with underlying measure  $\mu$ . The query  $\mathbf{q}$  is an arbitrary sequence of consecutive timepoints from the dynamical system. This proposition states that, when the context is sufficiently long, context parroting of an ergodic system preserves invariant values of the underlying dynamics. Context parroting thus represents an effective baseline for dynamical systems forecasting, because, in the limit of long context, it will preserve global properties like conditional distributions of values, Lyapunov exponents, or entropy production rates.

**Relationship to classical nonlinear forecasting.** We show in Appendix C.2 that, in various limits, context parroting reduces to two classical algorithms from nonlinear dynamics: the *simplex projection* technique and the *S-map* algorithm [71, 72]. Both approaches have their foundations in Takens’ embedding theorem, which states that time-delayed observables derived from a nonlinear dynamical system will recover key geometric properties of the underlying attractor [73]. However, unlike context parroting, which looks for the best matching motif, simplex projection tries to identify multiple matching motifs in the context and computes a weighted average as its forecast. This makes simplex projection more sensitive to the choice of the embedding dimension (i.e., the length of the motif  $D$ ), limiting the method to small embedding dimensions in practice [74].

## 4 Methods

**Datasets.** The dysts dataset provides a standardized benchmark of 135 low-dimensional chaotic systems, each defined by a set of ordinary differential equations between dimensionality three and six [75]. Every system is annotated with its largest Lyapunov exponent  $\lambda$ , an invariant characteristic of the underlying dynamics that quantifies the rate at which small perturbations grow over time. In chaotic systems, even minor errors rapidly compound over a characteristic timescale known as the Lyapunov time, defined as  $\tau \equiv \lambda^{-1}$ . As a result, highly chaotic systems (with small  $\tau$ ) are especially challenging to forecast.

**Models.** For time-series foundation models, we select Chronos<sub>base</sub> (200M parameters), its variant Chronos-Bolt<sub>base</sub> (205M parameters), Time-MoE<sub>large</sub> (200M parameters), and TimesFM-2.0 (500M parameters). All of these models are pretrained on massive amounts of real-world time series data (hundreds of billions of data points), which are often complemented by synthetic data to improve generalization. The three models encompass a wide array of design choices. Time-MoE and TimesFM employ decoder-only architectures, whereas Chronos adopts an encoder-decoder architecture. Chronos and Time-MoE use pointwise tokenization, whereas TimesFM chose patch tokenization. Time-MoE and TimesFM by default give point forecasts, whereas Chronos is designed to provide probabilistic forecasts with uncertainty quantification. Thus, for Chronos and Chronos-Bolt, we use the median prediction when evaluating forecast errors. An important parameter for these

foundation models is the maximum context length  $L_{\max}$ . Chronos has the shortest allowed context window at 512 data points, TimesFM-2.0 can handle 2048 data points in the context, and Time-MoE has the largest capacity at  $L_{\max} = 4096$ .

**Pipelines.** To evaluate different models' ability to zero-shot forecast dynamical systems, we generate a chaotic trajectory of length  $10^5$  for each of the 135 chaotic systems in dysts, with a granularity of 30 data points per Lyapunov time. For a given context length  $L$ , we randomly pick a length- $L$  segment from the chaotic trajectory and provide it to the model as the context. The model's task is to predict the next 300 data points (equivalent to 10 Lyapunov times) solely based on the context. We ask the model to make a univariate forecast on each dimension independently, which is then evaluated separately for each dimension. To obtain reliable statistics, we aggregate the results over all 135 chaotic systems, all dimensions, and 20 random initial conditions for each system.

**Metrics.** In line with previous research [75–78], we assess forecasting performance using two key metrics.

*Symmetric Mean Absolute Percentage Error (sMAPE).*

$$\text{sMAPE}(\mathbf{x}, \hat{\mathbf{x}}) \equiv 2 \frac{100}{T} \sum_{t=1}^T \frac{|\mathbf{x}_t - \hat{\mathbf{x}}_t|}{|\mathbf{x}_t| + |\hat{\mathbf{x}}_t|},$$

where the sequence  $\mathbf{x}_1, \mathbf{x}_2, \dots, \mathbf{x}_T$  denotes the ground truth, and  $\hat{\mathbf{x}}_1, \hat{\mathbf{x}}_2, \dots, \hat{\mathbf{x}}_T$  are the corresponding predictions made by the model.

*Valid Prediction Time (VPT).* This metric identifies the latest time step  $t_f$  before which the sMAPE remains below a predefined threshold  $\epsilon$ , as described in Vlachas et al. [79]. Formally:

$$\text{VPT} \equiv \text{argmax}_{t_f} \{t_f | \text{sMAPE}(\mathbf{x}_t, \hat{\mathbf{x}}_t) < \epsilon, \forall t < t_f\}.$$

We use  $\epsilon = 30$ , consistent with prior work [42, 78, 79].

In the appendix, we also show benchmark results using Mean Square Error (MSE) and Mean Absolute Error (MAE), two other metrics commonly used in the time series literature.

## 5 Results

### 5.1 Context parroting versus foundation models

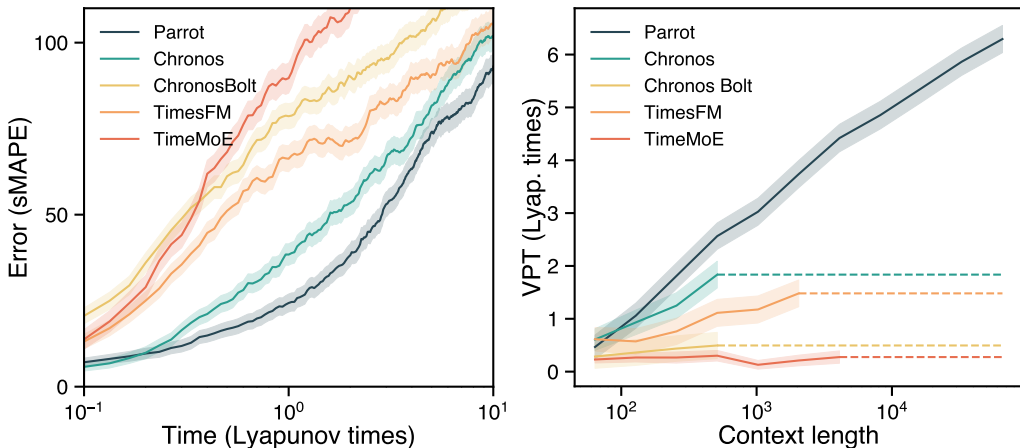


Figure 2: **Context parroting outperforms foundation models in zero-shot forecasting.** Left: Forecast error of each model as a function of the forecast horizon. The context length is set to 512 for all models. Right: Valid prediction time of each model as a function of the context length. Dashed lines indicate context lengths exceeding the maximum context window of the model. All results are averaged over the 135 chaotic systems in the dysts database, with 20 trajectories from random initial conditions for each system.

Here, we compare context parroting and foundation models in their ability to predict chaotic dynamics. Figure 2 shows each model’s forecasting error and valid prediction time. It is clear that context parroting is better than all foundation models in both metrics. In Fig. 9, we show that this remains true when benchmarked against MSE and MAE. Among foundation models, Chronos is the best performer in predicting chaotic systems, which is not surprising given that it utilizes parroting as a main forecasting strategy. Chronos’s tendency to context parrot arises from its distinct architecture as a language model that implicitly quantizes time series. As a result, Chronos is trained using cross-entropy loss, which incentivizes preservation of k-gram frequencies, ensuring repetition of sequences in the output and incentivizing generating diverse forecast samples consistent with the dynamical system’s underlying measure. In contrast, TimeMoE and TimesFM are trained using mean squared error loss, and so these models lose diversity and forecast the mean at long forecast horizons. Some representative forecasts from the foundation models are shown in Fig. 8.

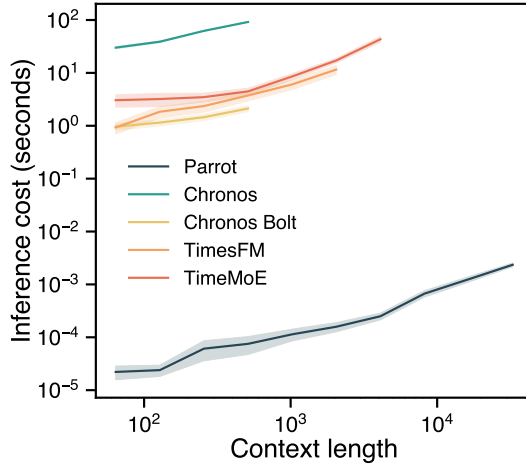


Figure 3: **Context parroting is computationally more efficient than foundation models.** There is generally a gap of five or six orders of magnitude between context parroting and foundation models. For each foundation model, context lengths from 64 to the maximum context window are considered. All inferences are performed with CPUs, and the forecast horizon is fixed to 300 steps.

Moreover, as we demonstrate in Fig. 3, the inference cost of context parroting is negligible compared to all foundation models (not to mention the substantial GPU time needed to pre-train foundation models). For example, there is an over six orders of magnitude gap between Chronos and context parroting for all context lengths. Combined with the fact that the performance of parroting is not sensitive to the choice of the embedding dimension  $D$  (Fig. 4), these results establish context parroting as a simple but hard-to-beat baseline for zero-shot forecasting of dynamical systems.

Figure 5 further explores the effect of context length on forecast accuracy. We find that longer context windows generally lead to better performance for both context parroting and Chronos. However, the longest context length Chronos can effectively utilize is 512 data points; anything beyond that will only increase inference cost without improving accuracy. This limit is determined by Chronos’s maximum context window chosen at pre-training. To be able to utilize longer context, Chronos must be retrained from scratch with much more data and compute. Context parroting, on the other hand, is happy to utilize context data of any length. Interestingly, Chronos outperforms context parroting on short contexts, which points to additional zero-shot learning strategies beyond parroting employed by Chronos. This is perhaps not surprising given that at short context length, the time series becomes effectively nonstationary, which is the strength of time-series foundation models. Moreover, even when restricted to parroting, Chronos can in principle dynamically choose the optimal embedding dimension  $D$  for each individual time series, giving it an advantage over parroting algorithms with a fixed  $D$ . It would be interesting to explicitly identify the mechanisms that enable Chronos to outperform parroting in this regime.

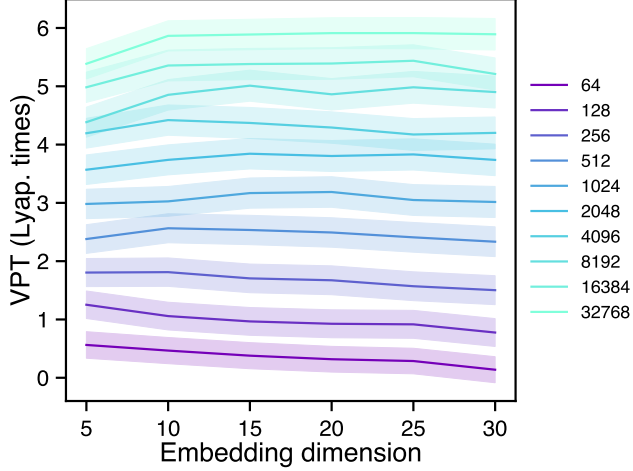


Figure 4: **Effect of the embedding dimension  $D$  on the forecast accuracy of context parrotting.** Overall, the valid prediction time stays consistent over a wide range of embedding dimension  $D$ . For short context windows, there is a slight advantage to small  $D$ . For long context windows, larger embedding dimensions are marginally better. This observation suggests potential improvements in the future that choose  $D$  adaptively based on factors such as context length.

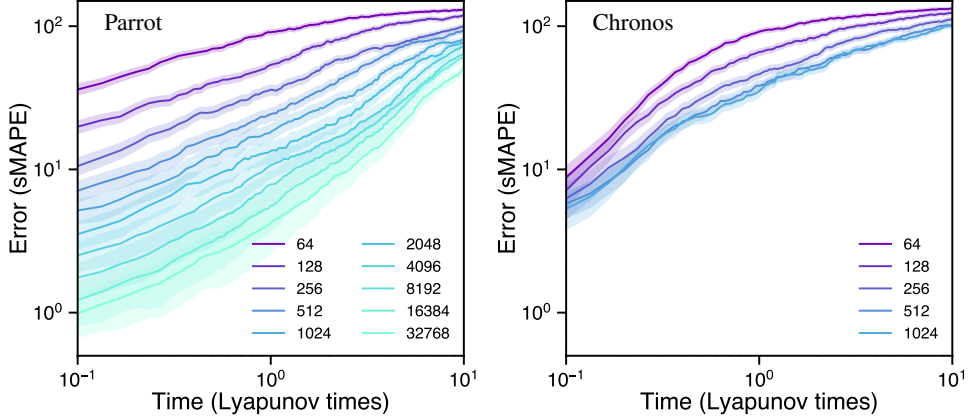


Figure 5: **Parrot can better utilize longer context data while Chronos does better for shorter contexts.** Each line represents a different context length. The performance of Chronos saturates once the context length exceeds 512 data points, whereas the accuracy of context parrotting keeps improving for longer context windows. Here we set the embedding dimension  $D = 10$  for the parrotting algorithm.

## 5.2 In-context neural scaling law

Liu et al. [61] reported an in-context neural scaling law for LLMs applied to learning dynamical systems, in which the one-step forecast error decreases algebraically with context length. However, it is unclear where this scaling law came from or why LLMs trained on text can be effective for time series without fine tuning. Here, we show that context parrotting naturally gives rise to the same in-context scaling law and provides geometric insights into its origin. Given the similarity between parrotting and the induction heads implemented by LLMs [62], the geometric explanation we develop next for context parrotting can conceivably be applied to LLMs and explain the observations in Liu et al. [61].

The left panel in Fig. 6 reproduces the power law relation between one-step forecast error (measured by sMAPE) and context length for the parrotting method. Why do longer context lengths enable better predictions of chaotic systems? This is because more context data allows the algorithm to

find better matching motifs, and a closely matched motif allows the parroted sequence to shadow the ground truth for longer. The overlap between the matching motifs can be measured by their Euclidean distance. For length- $D$  motifs, this is equivalent to embed the context trajectory in a  $D$ -dimensional delay-embedded space (mapping  $x_s$  to  $x_{s-D+1:s}$ ) and find the distance between the embedded last context point  $x_{t-D+1:t}$  and its nearest neighbor. The right panel in Fig. 6 shows the improving overlap explicitly, with the distance between the matching motifs decreasing algebraically with context length.

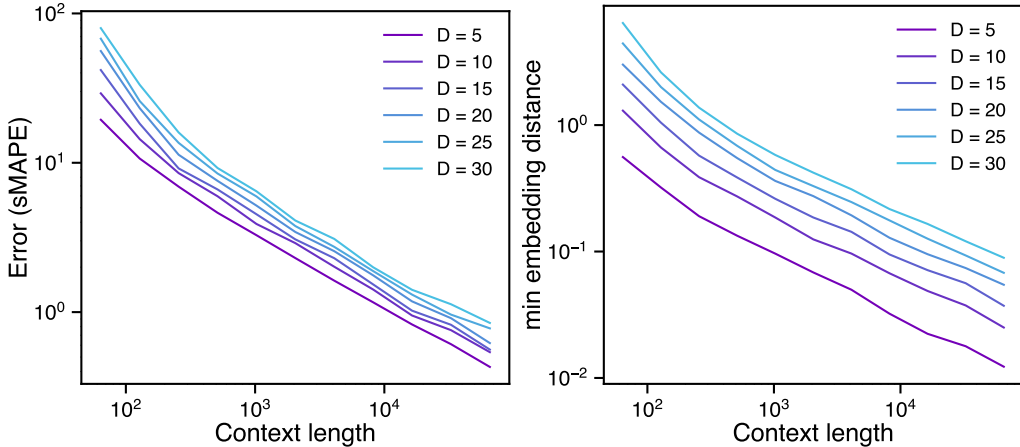


Figure 6: **Scaling laws with context length.** Left: One-step forecast error vs context length. The scaling follows a power law for all embedding dimensions considered. Smaller  $D$  is more accurate here because the use of the one-step forecast error. Larger  $D$  can be more accurate for longer forecasting horizons. Right: Euclidean distance between the last context motif  $x_{t-D+1:t}$  and its nearest neighbor in the  $D$ -dimensional delay-embedded space as a function of context length. Again, the scaling follows a power law for all  $D$ . The forecast accuracy is directly tied to the embedding distance: Smaller distances translate into better predictions. As the number of data points is increased, it becomes more and more likely that a context motif will land in the vicinity of the last context motif, and the correlation dimension of the chaotic attractor determines the rate of approach. In principle, infinite context length should give context parrotting infinite accuracy for any stationary and deterministic systems.

Why then does the minimum embedding distance follow a power law with context length,  $\ell \propto L^{-\alpha}$ ? We can link the scaling coefficient  $\alpha$  to the fractal dimension of the chaotic attractor. The correlation dimension  $d_{\text{cor}}$  of an attractor is defined as

$$d_{\text{cor}} \equiv \lim_{\epsilon, \epsilon' \rightarrow 0^+} \frac{\ln \left[ \frac{C(\epsilon)}{C(\epsilon')} \right]}{\ln \left( \frac{\epsilon}{\epsilon'} \right)},$$

where  $C(\epsilon)$  is the number of point pairs in the attractor that are within a given radius  $\epsilon$  from each other. In other words, if we plot  $C(\epsilon)$  against  $\epsilon$  on a log-log plot,  $d_{\text{cor}}$  would be the slope of the plotted line. Due to the ergodic property of chaotic attractors, the context trajectory can be seen as a random sample of the attractor. Longer context trajectory contains more samples, and the expected distance between two context points in a delay-embedded space decreases with context length as  $L^{-1/d_{\text{cor}}}$ . For example, for a two-dimensional attractor, the distance between two random points on the attractor will decrease as  $1/\sqrt{L}$ . Correlation dimension thus measures the speed at which the minimum embedding distance between points on an attractor can be reduced by including more samples, and higher dimensions require more points to reduce the distance to the same extent. Mathematically, we thus expect  $\alpha = 1/d_{\text{cor}}$ . However, numerically it is challenging to accurately estimate the scaling coefficient  $\alpha$  due to noise in the data. Nonetheless, in Fig. 7, we observe strong correlation between  $d_{\text{cor}}$  and  $1/\alpha$ , supporting our theoretical argument above.

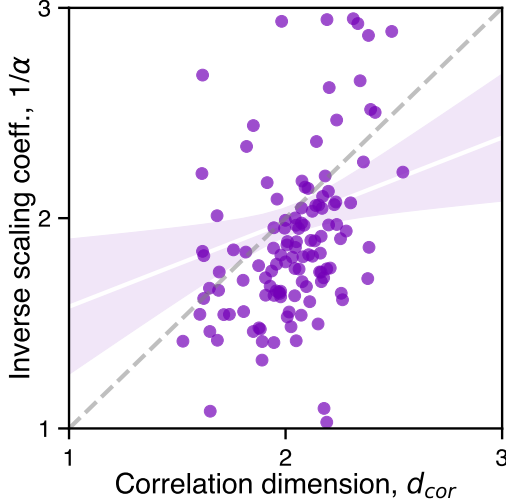


Figure 7: **Strong correlation between the inverse scaling coefficient  $1/\alpha$  and the correlation dimension  $d_{\text{cor}}$  of the chaotic attractor.** We estimate  $\alpha$  from the  $\ell$  vs  $L$  plot obtained with context parrotting at  $D = 10$ , where  $L$  ranges from  $2^6$  to  $2^{16}$ . This is done separately for each individual systems. Thus, each dot represents one of the 135 chaotic systems included in our benchmark. The Spearman rank-order correlation coefficient is  $0.44 \pm 0.08$  (bootstrapped standard error), and a linear regression with standard error range is underscored (shaded interval). The dashed line corresponds to an exact  $1 : 1$  scaling.

## 6 Conclusion and future directions

We find that a simple forecast strategy outperforms leading foundation models on dynamical systems forecasting, a critical task in scientific machine learning. This surprising finding exposes a limitation of current time-series foundation models as general-purpose time-series forecasters and highlights the need to further scale them or to fine-tune them for specific domains. It also suggests that accurately measuring the performance of foundation models can be difficult for scientific machine learning tasks, because simple, uninformative strategies like parrotting can effectively game both short- and long-term accuracy metrics.

Finding a simple but tough-to-beat baseline for a challenging task can encourage rethinking of the status quo, motivating better model architectures and baselines [80]. For example, identifying zero-shot learning strategies beyond parrotting can spur the development of next-generation foundation models and contribute to the debate on whether (or to what extent) large language models are stochastic parrots [81–84]. Context parrotting formalizes an explicit baseline to compare against in the time-series domain and can help discover beyond-parrotting strategies.

An important future direction is to generalize context parrotting to deal with non-stationary time series while keeping the simplicity and efficiency of the method. A promising avenue involves combining parrotting with a probabilistic model, such as a Gaussian Process, to account for nonstationary trends. Additionally, the diversity of long-term forecasts can be improved by allowing stochastic selection among multiple candidate forecasts. Once generalized, the non-stationary parrotting method can replace Naive and Seasonal Naive to serve as a more informative baseline for the zero-shot forecasting of general time series (weather, traffic, finance, etc.).

## Acknowledgments and Disclosure of Funding

YZ acknowledges support from the Omidyar Fellowship and NSF DMS 2436231. WG was supported by NSF DMS 2436233 and NSF CMMI 2440490. This project has been made possible in part by Grant No. DAF2023-329596 from the Chan Zuckerberg Initiative DAF, an advised fund of Silicon Valley Community Foundation.

## References

- [1] Steven L Brunton, Joshua L Proctor, and J Nathan Kutz. Discovering governing equations from data by sparse identification of nonlinear dynamical systems. *Proc. Natl. Acad. Sci. U.S.A.*, 113(15):3932–3937, 2016.
- [2] E Weinan. A proposal on machine learning via dynamical systems. *Commun. Math. Stat.*, 1(5):1–11, 2017.
- [3] Ricky TQ Chen, Yulia Rubanova, Jesse Bettencourt, and David K Duvenaud. Neural ordinary differential equations. *NeurIPS*, 31, 2018.
- [4] Jaideep Pathak, Brian Hunt, Michelle Girvan, Zhixin Lu, and Edward Ott. Model-free prediction of large spatiotemporally chaotic systems from data: A reservoir computing approach. *Phys. Rev. Lett.*, 120(2):024102, 2018.
- [5] Zongyi Li, Nikola Kovachki, Kamyar Azizzadenesheli, Burigede Liu, Kaushik Bhattacharya, Andrew Stuart, and Anima Anandkumar. Fourier neural operator for parametric partial differential equations. *arXiv:2010.08895*, 2020.
- [6] Renyi Chen and Molei Tao. Data-driven prediction of general hamiltonian dynamics via learning exactly-symplectic maps. In *International Conference on Machine Learning*, pages 1717–1727. PMLR, 2021.
- [7] Ian D Jordan, Piotr Aleksander Sokół, and Il Memming Park. Gated recurrent units viewed through the lens of continuous time dynamical systems. *Frontiers in computational neuroscience*, 15:678158, 2021.
- [8] Daniel J Gauthier, Erik Bollt, Aaron Griffith, and Wendson AS Barbosa. Next generation reservoir computing. *Nat. Commun.*, 12:5564, 2021.
- [9] Bryan Lim and Stefan Zohren. Time-series forecasting with deep learning: a survey. *Philosophical Transactions of the Royal Society A*, 379(2194):20200209, 2021.
- [10] George Em Karniadakis, Ioannis G Kevrekidis, Lu Lu, Paris Perdikaris, Sifan Wang, and Liu Yang. Physics-informed machine learning. *Nat. Rev. Phys.*, 3(6):422–440, 2021.
- [11] Matthew Levine and Andrew Stuart. A framework for machine learning of model error in dynamical systems. *Commun. Am. Math. Soc.*, 2(07):283–344, 2022.
- [12] Jonas Mikhæil, Zahra Monfared, and Daniel Durstewitz. On the difficulty of learning chaotic dynamics with rnns. *Advances in Neural Information Processing Systems*, 35:11297–11312, 2022.
- [13] Steven L Brunton, Marko Budisić, Eurika Kaiser, and J Nathan Kutz. Modern Koopman theory for dynamical systems. *SIAM Rev.*, 64(2):229–340, 2022.
- [14] Abhimanyu Das, Weihao Kong, Andrew Leach, Shaan Mathur, Rajat Sen, and Rose Yu. Long-term forecasting with tide: Time-series dense encoder. *arXiv:2304.08424*, 2023.
- [15] Aditi S Krishnapriyan, Alejandro F Queiruga, N Benjamin Erichson, and Michael W Mahoney. Learning continuous models for continuous physics. *Communications Physics*, 6(1):319, 2023.
- [16] Lu Yang, Xiuwen Sun, Boumediene Hamzi, Houman Owhadi, and Naiming Xie. Learning dynamical systems from data: A simple cross-validation perspective, part v: Sparse kernel flows for 132 chaotic dynamical systems. *Physica D: Nonlinear Phenomena*, 460:134070, 2024.
- [17] Rose Yu and Rui Wang. Learning dynamical systems from data: An introduction to physics-guided deep learning. *Proc. Natl. Acad. Sci. U.S.A.*, 121(27):e2311808121, 2024.
- [18] Kamyar Azizzadenesheli, Nikola Kovachki, Zongyi Li, Miguel Liu-Schiaffini, Jean Kossaifi, and Anima Anandkumar. Neural operators for accelerating scientific simulations and design. *Nat. Rev. Phys.*, pages 1–9, 2024.

[19] Manuel Brenner, Christoph Jürgen Hemmer, Zahra Monfared, and Daniel Durstewitz. Almost-linear rnns yield highly interpretable symbolic codes in dynamical systems reconstruction. *arXiv preprint arXiv:2410.14240*, 2024.

[20] Manuel Brenner, Elias Weber, Georgia Koppe, and Daniel Durstewitz. Learning interpretable hierarchical dynamical systems models from time series data. *arXiv preprint arXiv:2410.04814*, 2024.

[21] Matthew Ricci, Guy Pelc, Zoe Piran, Noa Moriel, and Mor Nitzan. Trendy: Temporal regression of effective non-linear dynamics. *arXiv preprint arXiv:2412.03496*, 2024.

[22] Yi He, Yiming Yang, Xiaoyuan Cheng, Hai Wang, Xiao Xue, Boli Chen, and Yukun Hu. Chaos meets attention: Transformers for large-scale dynamical prediction. *arXiv preprint arXiv:2504.20858*, 2025.

[23] Xiaoyuan Cheng, Yi He, Yiming Yang, Xiao Xue, Sibo Chen, Daniel Giles, Xiaohang Tang, and Yukun Hu. Learning chaos in a linear way. *arXiv preprint arXiv:2503.14702*, 2025.

[24] Lyudmila Grigoryeva, Hannah Lim Jing Ting, and Juan-Pablo Ortega. Infinite-dimensional next-generation reservoir computing. *Physical Review E*, 111(3):035305, 2025.

[25] Tyrus Berry and Suddhasattwa Das. Limits of learning dynamical systems. *SIAM Review*, 67(1):107–137, 2025.

[26] Boris N Oreshkin, Dmitri Carpov, Nicolas Chapados, and Yoshua Bengio. Meta-learning framework with applications to zero-shot time-series forecasting. In *Proceedings of the AAAI conference on artificial intelligence*, volume 35, pages 9242–9250, 2021.

[27] Azul Garza and Max Mergenthaler-Canseco. Timegpt-1. *arXiv:2310.03589*, 2023.

[28] Kashif Rasul, Arjun Ashok, Andrew Robert Williams, Arian Khorasani, George Adamopoulos, Rishika Bhagwatkar, Marin Bilos, Hena Ghonia, Nadhir Vincent Hassen, Anderson Schneider, et al. Lag-llama: Towards foundation models for time series forecasting. *arXiv:2310.08278*, 2023.

[29] Ming Jin, Shiyu Wang, Lintao Ma, Zhixuan Chu, James Y Zhang, Xiaoming Shi, Pin-Yu Chen, Yuxuan Liang, Yuan-Fang Li, Shirui Pan, et al. Time-LLM: Time series forecasting by reprogramming large language models. *arXiv:2310.01728*, 2023.

[30] Tian Zhou, Peisong Niu, Liang Sun, Rong Jin, et al. One fits all: Power general time series analysis by pretrained lm. *Advances in neural information processing systems*, 36:43322–43355, 2023.

[31] Nate Gruver, Marc Finzi, Shikai Qiu, and Andrew G Wilson. Large language models are zero-shot time series forecasters. *Advances in Neural Information Processing Systems*, 36, 2024.

[32] Samuel Dooley, Gurnoor Singh Khurana, Chirag Mohapatra, Siddartha V Naidu, and Colin White. Forecastpfn: Synthetically-trained zero-shot forecasting. *Advances in Neural Information Processing Systems*, 36, 2024.

[33] Yong Liu, Guo Qin, Xiangdong Huang, Jianmin Wang, and Mingsheng Long. Autotimes: Autoregressive time series forecasters via large language models. *arXiv:2402.02370*, 2024.

[34] Gerald Woo, Chenghao Liu, Akshat Kumar, Caiming Xiong, Silvio Savarese, and Doyen Sahoo. Unified training of universal time series forecasting transformers. *arXiv:2402.02592*, 2024.

[35] Abdul Fatir Ansari, Lorenzo Stella, Caner Turkmen, Xiyuan Zhang, Pedro Mercado, Huibin Shen, Oleksandr Shchur, Syama Sundar Rangapuram, Sebastian Pineda Arango, Shubham Kapoor, et al. Chronos: Learning the language of time series. *arXiv:2403.07815*, 2024.

[36] Mononito Goswami, Konrad Szafer, Arjun Choudhry, Yifu Cai, Shuo Li, and Artur Dubrawski. Moment: A family of open time-series foundation models. *arXiv:2402.03885*, 2024.

[37] Abhimanyu Das, Weihao Kong, Rajat Sen, and Yichen Zhou. A decoder-only foundation model for time-series forecasting. In *Forty-first International Conference on Machine Learning*, 2024.

[38] Yuxuan Liang, Haomin Wen, Yuqi Nie, Yushan Jiang, Ming Jin, Dongjin Song, Shirui Pan, and Qingsong Wen. Foundation models for time series analysis: A tutorial and survey. *arXiv:2403.14735*, 2024.

[39] Xiaoming Shi, Shiyu Wang, Yuqi Nie, Dianqi Li, Zhou Ye, Qingsong Wen, and Ming Jin. Time-moe: Billion-scale time series foundation models with mixture of experts. *arXiv:2409.16040*, 2024.

[40] Zheng-Meng Zhai, Jun-Yin Huang, Benjamin D Stern, and Ying-Cheng Lai. Reconstructing dynamics from sparse observations with no training on target system. *arXiv:2410.21222*, 2024.

[41] Yong Liu, Guo Qin, Zhiyuan Shi, Zhi Chen, Caiyin Yang, Xiangdong Huang, Jianmin Wang, and Mingsheng Long. Sundial: A family of highly capable time series foundation models. *arXiv:2502.00816*, 2025.

[42] Yuanzhao Zhang and William Gilpin. Zero-shot forecasting of chaotic systems. *arXiv:2409.15771*, 2024.

[43] John A Miller, Mohammed Aldosari, Farah Saeed, Nasid Habib Barna, Subas Rana, I Budak Arpinar, and Ninghao Liu. A survey of deep learning and foundation models for time series forecasting. *arXiv:2401.13912*, 2024.

[44] Makoto Takamoto, Timothy Praditia, Raphael Leiteritz, Daniel MacKinlay, Francesco Alesiani, Dirk Pflüger, and Mathias Niepert. Pdebench: An extensive benchmark for scientific machine learning. *Advances in Neural Information Processing Systems*, 35:1596–1611, 2022.

[45] Liu Yang, Siting Liu, Tingwei Meng, and Stanley J Osher. In-context operator learning with data prompts for differential equation problems. *Proc. Natl. Acad. Sci. U.S.A.*, 120(39):e2310142120, 2023.

[46] Md Ashiqur Rahman, Robert Joseph George, Mogab Elleithy, Daniel Leibovici, Zongyi Li, Boris Bonev, Colin White, Julius Berner, Raymond A Yeh, Jean Kossaifi, et al. Pretraining codomain attention neural operators for solving multiphysics pdes. *arXiv:2403.12553*, 2024.

[47] Shashank Subramanian, Peter Harrington, Kurt Keutzer, Wahid Bhimji, Dmitriy Morozov, Michael W Mahoney, and Amir Gholami. Towards foundation models for scientific machine learning: Characterizing scaling and transfer behavior. *Advances in Neural Information Processing Systems*, 36, 2024.

[48] Maximilian Herde, Bogdan Raonić, Tobias Rohner, Roger Käppeli, Roberto Molinaro, Emmanuel de Bézenac, and Siddhartha Mishra. Poseidon: Efficient foundation models for pdes. *arXiv:2405.19101*, 2024.

[49] Michael McCabe, Bruno Régaldo-Saint Blancard, Liam Parker, Ruben Ohana, Miles Cranmer, Alberto Bietti, Michael Eickenberg, Siavash Golkar, Geraud Krawezik, Francois Lanusse, et al. Multiple physics pretraining for spatiotemporal surrogate models. *Advances in Neural Information Processing Systems*, 37:119301–119335, 2024.

[50] Amin Totounferoush, Serge Kotchourko, Michael W Mahoney, and Steffen Staab. Paving the way for scientific foundation models: enhancing generalization and robustness in pdes with constraint-aware pre-training. *arXiv preprint arXiv:2503.19081*, 2025.

[51] Wenhui Cui, Woojae Jeong, Philipp Thölke, Takfarinas Medani, Karim Jerbi, Anand A Joshi, and Richard M Leahy. Neuro-gpt: Towards a foundation model for eeg. In *2024 IEEE International Symposium on Biomedical Imaging (ISBI)*, pages 1–5. IEEE, 2024.

[52] Josue Ortega Caro, Antonio H de O Fonseca, Christopher Averill, Syed A Rizvi, Matteo Rosati, James L Cross, Prateek Mittal, Emanuele Zappala, Daniel Levine, Rahul M Dhodapkar, et al. Brainlm: A foundation model for brain activity recordings. *bioRxiv*, pages 2023–09, 2023.

[53] Kaden McKeen, Laura Oliva, Sameer Masood, Augustin Toma, Barry Rubin, and Bo Wang. Ecg-fm: An open electrocardiogram foundation model. *arXiv preprint arXiv:2408.05178*, 2024.

[54] Tung Nguyen, Johannes Brandstetter, Ashish Kapoor, Jayesh K Gupta, and Aditya Grover. Climax: A foundation model for weather and climate. *arXiv:2301.10343*, 2023.

[55] Cristian Bodnar, Wessel P Bruinsma, Ana Lucic, Megan Stanley, Johannes Brandstetter, Patrick Garvan, Maik Riechert, Jonathan Weyn, Haiyu Dong, Anna Vaughan, et al. Aurora: A foundation model of the atmosphere. *arXiv:2405.13063*, 2024.

[56] Jared Kaplan, Sam McCandlish, Tom Henighan, Tom B Brown, Benjamin Chess, Rewon Child, Scott Gray, Alec Radford, Jeffrey Wu, and Dario Amodei. Scaling laws for neural language models. *arXiv:2001.08361*, 2020.

[57] Ben Sorscher, Robert Geirhos, Shashank Shekhar, Surya Ganguli, and Ari Morcos. Beyond neural scaling laws: beating power law scaling via data pruning. *Advances in Neural Information Processing Systems*, 35:19523–19536, 2022.

[58] Yasaman Bahri, Ethan Dyer, Jared Kaplan, Jaehoon Lee, and Utkarsh Sharma. Explaining neural scaling laws. *Proc. Natl. Acad. Sci. U.S.A.*, 121(27):e2311878121, 2024.

[59] Qingren Yao, Chao-Han Huck Yang, Renhe Jiang, Yuxuan Liang, Ming Jin, and Shirui Pan. Towards neural scaling laws for time series foundation models. *arXiv:2410.12360*, 2024.

[60] Jordan Hoffmann, Sebastian Borgeaud, Arthur Mensch, Elena Buchatskaya, Trevor Cai, Eliza Rutherford, Diego de Las Casas, Lisa Anne Hendricks, Johannes Welbl, Aidan Clark, et al. Training compute-optimal large language models. *arXiv:2203.15556*, 2022.

[61] Toni JB Liu, Nicolas Boullé, Raphaël Sarfati, and Christopher J Earls. Llms learn governing principles of dynamical systems, revealing an in-context neural scaling law. *arXiv:2402.00795*, 2024.

[62] Catherine Olsson, Nelson Elhage, Neel Nanda, Nicholas Joseph, Nova DasSarma, Tom Henighan, Ben Mann, Amanda Askell, Yuntao Bai, Anna Chen, et al. In-context learning and induction heads. *arXiv:2209.11895*, 2022.

[63] Johannes Von Oswald, Eyyvind Niklasson, Ettore Randazzo, João Sacramento, Alexander Mordvintsev, Andrey Zhmoginov, and Max Vladymyrov. Transformers learn in-context by gradient descent. In *International Conference on Machine Learning*, pages 35151–35174. PMLR, 2023.

[64] Gautam Reddy. The mechanistic basis of data dependence and abrupt learning in an in-context classification task. *arXiv:2312.03002*, 2023.

[65] Ezra Edelman, Nikolaos Tsilivis, Benjamin Edelman, Eran Malach, and Surbhi Goel. The evolution of statistical induction heads: In-context learning markov chains. *Advances in Neural Information Processing Systems*, 37:64273–64311, 2024.

[66] Siyu Chen, Heejune Sheen, Tianhao Wang, and Zhuoran Yang. Unveiling induction heads: Provable training dynamics and feature learning in transformers. In *The Thirty-eighth Annual Conference on Neural Information Processing Systems*, 2024.

[67] Ang Lv, Ruobing Xie, Xingwu Sun, Zhanhui Kang, and Rui Yan. Language models" grok" to copy. *arXiv preprint arXiv:2409.09281*, 2024.

[68] Yanda Chen, Chen Zhao, Zhou Yu, Kathleen McKeown, and He He. Parallel structures in pre-training data yield in-context learning. In *62nd Annual Meeting of the Association for Computational Linguistics, ACL 2024*, pages 8582–8592. Association for Computational Linguistics (ACL), 2024.

[69] Nitish Shirish Keskar, Bryan McCann, Lav R Varshney, Caiming Xiong, and Richard Socher. Ctrl: A conditional transformer language model for controllable generation. *arXiv preprint arXiv:1909.05858*, 2019.

[70] Oussama Zekri, Ambroise Odonnat, Abdelhakim Benechehab, Linus Bleistein, Nicolas Boullé, and Ievgen Redko. Large language models as markov chains. *arXiv preprint arXiv:2410.02724*, 2024.

[71] George Sugihara and Robert M May. Nonlinear forecasting as a way of distinguishing chaos from measurement error in time series. *Nature*, 344(6268):734–741, 1990.

[72] George Sugihara. Nonlinear forecasting for the classification of natural time series. *Philosophical Transactions of the Royal Society of London. Series A: Physical and Engineering Sciences*, 348(1688):477–495, 1994.

[73] Jeremy P Huke. Embedding nonlinear dynamical systems: A guide to takens’ theorem. 2006.

[74] Chun-Wei Chang, Masayuki Ushio, and Chih-hao Hsieh. Empirical dynamic modeling for beginners. *Ecological research*, 32:785–796, 2017.

[75] William Gilpin. Chaos as an interpretable benchmark for forecasting and data-driven modelling. *NeurIPS*, 34, 2021.

[76] Rob J Hyndman and Anne B Koehler. Another look at measures of forecast accuracy. *International journal of forecasting*, 22(4):679–688, 2006.

[77] Spyros Makridakis, Evangelos Spiliotis, and Vassilios Assimakopoulos. The m5 competition: Background, organization, and implementation. *International Journal of Forecasting*, 38(4):1325–1336, 2022.

[78] William Gilpin. Model scale versus domain knowledge in statistical forecasting of chaotic systems. *Phys. Rev. Research*, 5(4):043252, 2023.

[79] Pantelis R Vlachas, Jaideep Pathak, Brian R Hunt, Themistoklis P Sapsis, Michelle Girvan, Edward Ott, and Petros Koumoutsakos. Backpropagation algorithms and reservoir computing in recurrent neural networks for the forecasting of complex spatiotemporal dynamics. *Neural. Netw.*, 126:191–217, 2020.

[80] Sanjeev Arora, Yingyu Liang, and Tengyu Ma. A simple but tough-to-beat baseline for sentence embeddings. In *International conference on learning representations*, 2017.

[81] Emily M Bender, Timnit Gebru, Angelina McMillan-Major, and Shmargaret Shmitchell. On the dangers of stochastic parrots: Can language models be too big? In *Proceedings of the 2021 ACM conference on fairness, accountability, and transparency*, pages 610–623, 2021.

[82] Melanie Mitchell and David C Krakauer. The debate over understanding in ai’s large language models. *Proc. Natl. Acad. Sci. U.S.A.*, 120(13):e2215907120, 2023.

[83] Sanjeev Arora and Anirudh Goyal. A theory for emergence of complex skills in language models. *arXiv:2307.15936*, 2023.

[84] R Thomas McCoy, Shunyu Yao, Dan Friedman, Mathew D Hardy, and Thomas L Griffiths. Embers of autoregression show how large language models are shaped by the problem they are trained to solve. *Proc. Natl. Acad. Sci. U.S.A.*, 121(41):e2322420121, 2024.

[85] Yao-Hung Hubert Tsai, Shaojie Bai, Makoto Yamada, Louis-Philippe Morency, and Ruslan Salakhutdinov. Transformer dissection: An unified understanding for transformer’s attention via the lens of kernel. In *Proceedings of the Conference on Empirical Methods in Natural Language Processing*, 2019.

[86] P Walters. An introduction to ergodic theory. *Springer-Verlag*, 1982.

[87] Richard C Bradley. Basic properties of strong mixing conditions. a survey and some open questions. *Probability Surveys*, 2:107–144, 2005.

[88] Jianqing Fan and Qiwei Yao. *Nonlinear time series: nonparametric and parametric methods*. Springer Science & Business Media, 2008.

[89] Kunio Takezawa. *Introduction to nonparametric regression*. John Wiley & Sons, 2005.

## A Sample predictions from foundation models

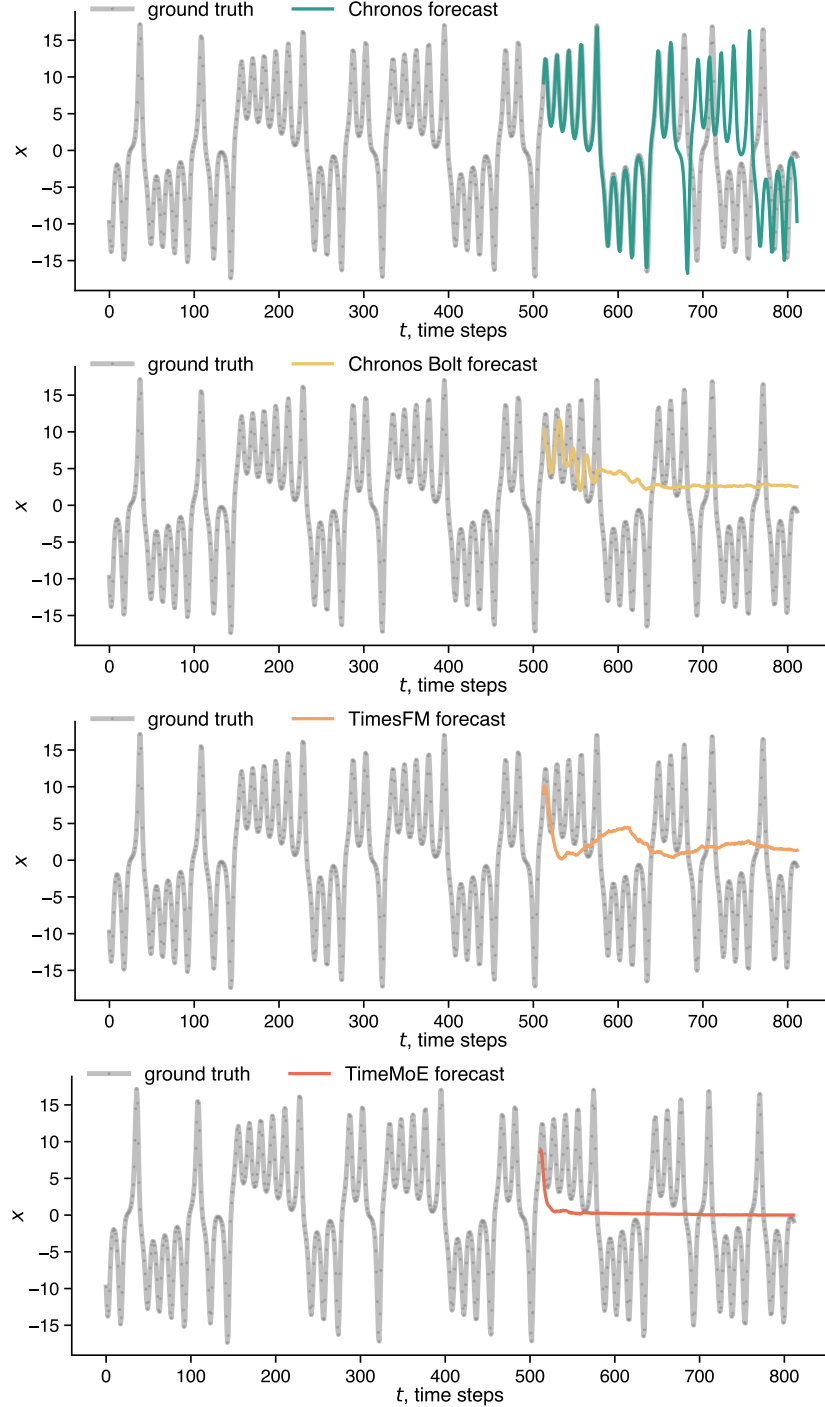


Figure 8: **Example forecasts on a chaotic system from foundation models.** This is the same task as presented in Fig. 1 (predicting the  $x$  variable of the Lorenz system based on a short context trajectory with 512 data points). Chronos does extremely well with a parroting strategy. The other models perform comparatively poorly and all exhibit a tendency to underestimate the oscillations (e.g., by quickly converging towards the mean). This is a general trend that we consistently observe across different chaotic systems and initial conditions.

## B Benchmarking with other metrics

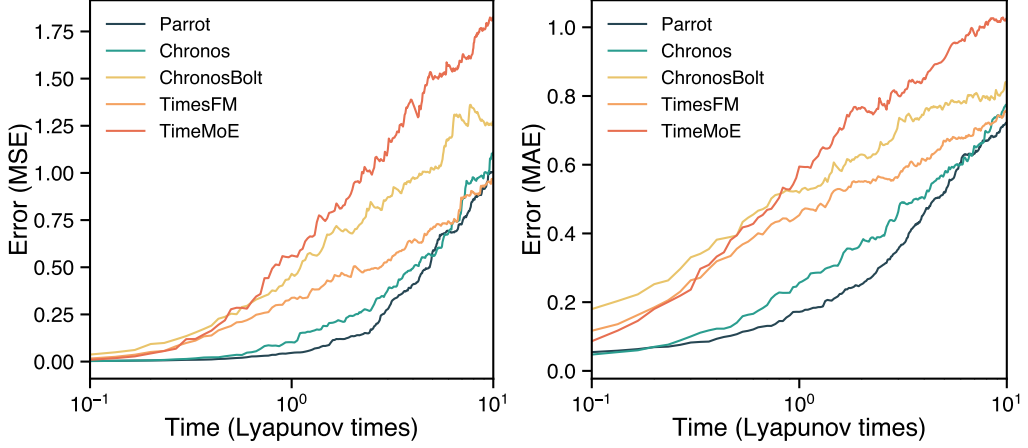


Figure 9: **Context parrotting outperforms foundation models in zero-shot forecasting.** Same setup as in Fig. 2, but with the forecast error measured by MSE (left) and MAE (right).

## C Context parrotting

### C.1 Discrete-token parrotting

For fully-discrete tokens, an  $L^{th}$  order Markov chain fit to the context has the form

$$p(\mathbf{y}|\mathbf{q}) = \frac{\#\{j : (x_{j-(L-1):j} = \mathbf{q}) \wedge (x_{j+1:j+H} = \mathbf{y})}{\sum_{\mathbf{y}'} \#\{i : (x_{j-(L-1):j} = \mathbf{q}) \wedge (x_{j+1:j+H} = \mathbf{y}')\}} \quad (3)$$

where the overall context has length  $C$ , and the Markov chain conditions the  $H < C$  future tokens on the  $L < C$  preceding tokens. The index  $j$  runs over all contiguous sequences of length  $L + H$  in the context,  $j \in \{L - 1, L, \dots, C - H - 2, C - H - 1\}$ . The vector  $\mathbf{q} \in \mathbb{R}^L$  represents the query, and the vector  $\mathbf{y} \in \mathbb{R}^H$  represents the prediction in response to this query. Eq. 3 simply counts the number of token sequences of length  $H + L$  that start with a given sequence of  $L$  query tokens. A maximum-likelihood estimator derived from this model always samples the highest-likelihood sequence  $\mathbf{y}$ ,

$$\hat{\mathbf{y}}_{\text{MLE}}(\mathbf{q}) = \text{argmax}_{\mathbf{y}} \log p(\mathbf{y}|\mathbf{q})$$

However, this estimator may be unstable due to the appearance of queries  $\mathbf{q}$  not seen in the context, motivating the use of *token smoothing*, in which Eq. 3 is replaced by the distribution

$$p(\mathbf{y}|\mathbf{q}) = \frac{\#\{j : (x_{j-(L-1):j} = \mathbf{q}) \wedge (x_{j+1:j+H} = \mathbf{y}) + \alpha}{\sum_{\mathbf{y}'} (\#\{i : (x_{j-(L-1):j} = \mathbf{q}) \wedge (x_{j+1:j+H} = \mathbf{y}') + \alpha)} \quad (4)$$

with increasing values of the parameter  $\alpha$  causing predictions to converge to a uniform sample over possible predictions  $\mathbf{y}$ . The parameter value  $\alpha = 0$  reduces to no smoothing, while  $\alpha = 0.5$  corresponds to the Jeffreys prior and  $\alpha = 1$  corresponds to Laplace's rule of succession.

### C.2 Continuous-token parrotting

A more general time series model treats tokens as continuous-valued. Some time series foundation models like Chronos use quantile binning to discretize time series values, allowing the direct use of discrete-token architectures [35]. However, many time series models assume effective continuity in token values, and we favor a continuous formulation in order to highlight connections to dynamical systems theory.

To model continuous-valued tokens directly, we replace the discrete count in §C.1 with a kernel-weighted estimate over all past subsequences. Let  $\{\mathbf{x}_t\}_{t=1}^C$  be a univariate or multivariate time series.

For context length  $L$  and prediction horizon  $H$ , the Nadaraya–Watson estimate of the conditional density is

$$\hat{p}(\mathbf{y} \mid \mathbf{q}) = \frac{\sum_{j=L}^{C-H} K_h(\mathbf{q}, \mathbf{x}_{j-(L-1):j}) K_h(\mathbf{y}, \mathbf{x}_{j+1:j+H})}{\sum_{j=L}^{C-H} K_h(\mathbf{q}, \mathbf{x}_{j-(L-1):j})}, \quad (5)$$

where  $K_h(\mathbf{u}, \mathbf{v}) = h^{-d} K((\mathbf{u} - \mathbf{v})/h)$  is a symmetric kernel with bandwidth  $h$  in dimension  $d = L \cdot \dim(x_t)$ . Assuming mean-squared error as a distance function in sequence space, we use a Gaussian kernel

$$K_h(\mathbf{u}, \mathbf{v}) = \frac{1}{(2\pi h^2)^{d/2}} \exp\left(-\frac{\|\mathbf{u} - \mathbf{v}\|^2}{2h^2}\right)$$

In practice, we drop the second kernel on  $\mathbf{y}$  in Eq. 5 and write the conditional mean predictor

$$\hat{\mathbf{y}}(\mathbf{q}) = \sum_{j=L}^{C-H} w(\mathbf{q}, \mathbf{x}_{j-(L-1):j}) \mathbf{x}_{j+1:j+H} \quad (6)$$

where we have isolated a term corresponding to the weight of each sequence,

$$w(\mathbf{q}, \mathbf{z}) \equiv \frac{K_h(\mathbf{q}, \mathbf{z})}{\sum_{j=L}^{C-H} K_h(\mathbf{q}, \mathbf{x}_{j-(L-1):j})}.$$

**Nearest-neighbor and global average limits.** The bandwidth  $h$  plays the role of a smoothing parameter (analogous to  $\alpha$  in Eq. 4). As  $h \rightarrow 0$  the scheme approximates a single-nearest neighbor parrot, while as  $h \rightarrow \infty$  it converges to a global average over all sequences.

**Connection to attention.** If one takes

$$K(\mathbf{u}, \mathbf{v}) = \exp(\mathbf{u}^\top \mathbf{v} / \tau),$$

then Eq. 6 recovers a simplified form of softmax-attention, with the temperature hyperparameter  $\tau$  controlling smoothness. In this view, the continuous parrotting scheme is a kernel-regression analogue of discrete  $k$ -gram smoothing [85].

**$k$ -nearest-neighbor limit.** We define a set  $\text{Top}_k$  corresponding to a subset of the possible values of the index  $j \in \{L, L+1, \dots, C-H-1, C-H\}$ . The  $k$  elements of  $\text{Top}_k$  correspond to the indices  $j$  that produce the  $k$  largest values of  $w(\mathbf{q}, \mathbf{x}_{j-(L-1):j})$  across all values of  $j$ . We compute a simple average of these  $k$  closest matches

$$\hat{\mathbf{y}}(\mathbf{q}) = \frac{1}{k} \sum_{j \in \text{Top}_k} w(\mathbf{q}, \mathbf{x}_{j-(L-1):j}) \mathbf{x}_{j+1:j+H} \quad (7)$$

yielding a  $k$ -nearest-neighbors parrotting scheme. As  $k$  increases, this estimator interpolates between exact parrotting ( $k = 1$ ) and global average ( $k \rightarrow C$ ).

**Simplex projection.** Simplex projection, a classical forecasting method in nonlinear dynamics, corresponds to the special case  $H = 1$  (single step prediction),  $k = L + 1$  in Eq. 7. The condition  $k = L + 1$  represents the minimal number of affinely independent neighbors needed to triangulate a point in an  $L$ -dimensional space [71].

In simplex projection, the query  $\mathbf{q}$  is interpreted as a time-delay embedding of the time series observable  $\mathbf{x}$ . Takens' theorem argues that, under mild conditions, a finite number of time delay embeddings of an observable drawn from a deterministic ergodic system will be diffeomorphic (smoothly mappable) to the full-state dynamics [73]. Because simplex projection uses only neighbor identities, and not absolute distances, to weight context points, a delay embedding is sufficient to calculate the appropriate weights.

**S-map forecasts.** Another common nonlinear forecasting technique retains all terms in the sum Eq. 6, but instead performs a nonlinear weighting of the form

$$K_\theta(\mathbf{u}, \mathbf{v}) = \exp(-\theta \|\mathbf{u} - \mathbf{v}\| / \bar{d})$$

where the scale parameter  $\bar{d}$  is determined by the distribution of distances among queries and points in the context. In practice, this parameter is often set to the mean pairwise distance among all sequences

of length  $L$  in the context. The optimal value of the hyperparameter  $\theta$  increases as the underlying dynamics become more strongly nonlinear [72]. We note that, in the classical formulation of the S-map, a locally-linear model is fit based on all sequences of length  $L + H$  seen in the context, while here we use the Nadaraya–Watson estimator in order to emphasize connections to modern kernel regression.

### C.3 Invariants of motion

For ergodic dynamical systems in continuous time, there exists a natural measure  $\mu(\mathbf{x})$  such that, for certain observables  $F(\mathbf{x})$ , the following condition almost surely holds,

$$\mathbb{E}_\mu[F] \equiv \lim_{T \rightarrow \infty} \frac{1}{T} \int_0^T F(\mathbf{x}) = \int F(\mathbf{x}) d\mu(\mathbf{x}) = \text{constant}$$

where the second equality arises from the Birkhoff ergodic theorem [86].

We use the following convention for expectation values of sequences and single tokens; the expectation  $\mathbb{E}_\mu[\mathbf{x}_{t:t+T}]$  refers to the expected value of the sequence  $\mathbf{x}_{t:t+T}$  given pointwise measure  $\mu$ . We note that, for deterministic dynamical systems, once a given point is sampled on the attractor with measure  $\mu(\mathbf{x}_t)$ , subsequent points have delta function conditional probability on the first point. Thus, we use the convention  $\mu(\mathbf{x}_t) = \mu(\mathbf{x}_{t:t+T})$  and we use the measure to refer to both the probability of a given timepoint, or a sequence of arbitrary length originating from that timepoint.

**Proposition.** Under appropriate kernel conditions,

$$\lim_{C \rightarrow \infty} \mathbb{E}_p[F(\mathbf{y})|\mathbf{q}] = \mathbb{E}_\mu[F(\mathbf{x})]$$

where  $C$  is the context length for a Nadaraya–Watson estimator  $p$ ,  $F(\mathbf{y})$  is an estimate on a sequence  $\mathbf{y}$  of an invariant property of an ergodic dynamical system with measure  $\mu$ , and  $\mathbf{q}$  is an arbitrary sequence of consecutive timepoints from the dynamical system. This proposition states that, when the context is sufficiently long, a Nadaraya–Watson estimator of an ergodic system preserves the invariant values of the underlying dynamics.

**Derivation.** We start with the definition of the dynamical average,

$$\mathbb{E}_\mu[F] = \int F(\mathbf{x}) d\mu(\mathbf{x})$$

Inserting Eq. 5 into this expression,

$$\mathbb{E}_\mu[F(\mathbf{y})|\mathbf{q}] = \frac{\sum_{j=L}^{C-H} K_h(\mathbf{q}, \mathbf{x}_{j-(L-1):j}) \int F(\mathbf{y}) K_h(\mathbf{y}, \mathbf{x}_{j+1:j+H}) d\mu(\mathbf{y})}{\sum_{j=L}^{C-H} K_h(\mathbf{q}, \mathbf{x}_{j-(L-1):j})},$$

We multiply both the numerator and denominator by  $1/C$  and take the limit  $C \rightarrow \infty$ , in order to convert the summations to expectations,

$$\lim_{C \rightarrow \infty} \mathbb{E}_\mu[F(\mathbf{y})|\mathbf{q}] = \frac{\mathbb{E}_\mu[K_h(\mathbf{q}, \mathbf{x}_{\leftarrow}) \int F(\mathbf{y}) K_h(\mathbf{y}, \mathbf{x}_{\rightarrow}) d\mu(\mathbf{y})]}{\mathbb{E}_\mu[K_h(\mathbf{q}, \mathbf{x}_{\leftarrow})]},$$

where  $\mathbf{x}_{\leftarrow}$  represents the first  $L$  points of random lookback window of length  $L + H$  sampled from the underlying dynamical system, while  $\mathbf{x}_{\rightarrow}$  denotes the next  $H$  timepoints. In practice, this corresponds to a time series of  $L + H$  points generated by simulating the dynamics starting at a point on the attractor randomly-sampled according to the measure  $\mu$ .

If we take the limit  $h \rightarrow 0$ , then the kernel  $K_h$  becomes a delta function, yielding

$$\lim_{h \rightarrow 0} \lim_{C \rightarrow \infty} \mathbb{E}_\mu[F(\mathbf{y})|\mathbf{q}] = \mathbb{E}_\mu[F(\mathbf{x}_{\rightarrow})|\mathbf{x}_{\leftarrow} = \mathbf{q}]$$

If the measure  $\mu$  is ergodic, then the conditional expectation of an invariant  $F$  given any query  $\mathbf{q}$  is simply its unconditional expectation,

$$\lim_{h \rightarrow 0} \lim_{C \rightarrow \infty} \mathbb{E}_\mu[F(\mathbf{y})|\mathbf{q}] = \mathbb{E}_\mu[F(\mathbf{x})]$$

#### C.4 Scaling laws

For a time series  $\mathbf{x}_{1:T}$  with autocorrelation given by

$$|\text{Corr}(\mathbf{x}_t, \mathbf{x}_{t+\tau})| \leq Ce^{-\alpha\tau}, \quad \alpha > 0$$

the expected forecast error scales as

$$\mathbb{E}[\|\hat{\mathbf{y}} - \mathbf{y}\|^2] \sim e^{-\alpha L}, \quad L \rightarrow \infty.$$

Thus, under exponential decay of correlations (mixing), the amount of information about future states in a length- $L$  context window saturates exponentially quickly [87]. Thus, forecasts derived from increasingly large context windows converge exponentially quickly to optimal conditional forecasts under the invariant measure  $\mu$ .

Under standard smoothness conditions [88, 89], the forecast error also exhibits a standard bias-variance tradeoff of the form

$$\mathbb{E}[\|\hat{\mathbf{y}} - \mathbf{y}\|^2] = \mathcal{O}(h^4) + \mathcal{O}\left(\frac{1}{Ch^{L+H}}\right).$$

The optimal width of the kernel thus scales as,

$$h_{\text{opt}} \sim C^{-1/(4+L+H)}$$